Effect of Wind Velocity on Smoldering Ignition of Moist Pine Needles by a Glowing Firebrand

Wei Fang, State Key Laboratory of Fire Science, University of Science and Technology of China, Hefei 230026 Anhui, China

Jiuling Yang 🆔 *, School of Engineering, Sichuan Normal University, Chengdu 610101 Sichuan, China*

Haixiang Chen 🆔*, Linhe Zhang, Pengcheng Guo and Yukui Yuan, State Key Laboratory of Fire Science, University of Science and Technology of China, Hefei 230026 Anhui, China*

Abstract. Firebrand ignition of wildland fuels is an important pathway of initiation and propagation of wildland and wildland-urban interface fires. The ambient wind plays an important role in smouldering ignition of wildland fuels by firebrands, but its influence is poorly stated. In this work, the effect of ambient wind on the ignition of a moist pine needle fuel bed by a glowing firebrand was investigated. Two ignition outcomes, smouldering or failed ignition, were observed. Wind was found to have a significant impact on the ignition process by affecting the glowing combustion state of the firebrand. As the wind velocity increased from zero to 4 m/s, the smouldering ignition probability firstly increased and then decreased, while the smouldering ignition delay time decreased. Under the same wind conditions, the ignition probability decreased while the smouldering ignition delay time increased as the fuel moisture content increased from 5.9% to 53.2%. A theoretical model based on the glowing combustion rate of firebrand and heat transfer between the firebrand and the fuel bed under the effect of wind was proposed. The model predicted the variation trend of the smouldering ignition delay time with the wind velocity well when FMC was less than 20%, but poor at higher FMC. It also predicted that the square root of ignition delay time had a good linear relationship with FMC. This work is a step forward in understanding of spot fires initiated by glowing firebrands.

* Correspondence should be addressed to: Haixiang Chen, E-mail: hxchen@ustc.edu.cn

1. Introduction

Research highlights that the most economically or socially devastating wildfires are concentrated in wildland-urban interface (WUI) areas [1]. Increase of WUI communities, coupled with global climate change, land use, etc. has resulted in wildfires of increasing number, severity, magnitude, and impact on humans [1–3].

Spotting ignition by firebrands is an important pathway of the initiation and propagation of wildfires and WUI fires [4, 5]. Ignition due to firebrands is a complex process involving multiple physical and chemical processes in the solid and gas phases [6] and has received intensive investigation in literature. Numerous works have examined the ability of single and in some cases multiple firebrands to ignite various fuels [7–11]. It is found that ambient wind, fuel moisture content (FMC) as well as firebrand size and state are the main factors that determine the ignition outcomes.

As for firebrand state, firebrands could be either in flaming or glowing state when landing on the receipt fuels. Although flaming firebrands are more successful than glowing firebrands in igniting fuel beds and starting spot fires, firebrands are in a glowing combustion state in most spotting fire scenarios [12, 13].

When a glowing firebrand ignites a fuel bed, the ambient wind has an important influence. Several studies have reported the effect of wind velocity on glowing firebrand ignition of substrate fuels [7, 8, 11]. Ganteaume et al. [7] found that the flaming ignition probability of Mediterranean wildland fuels caused by glowing firebrands increases with wind velocity, suggesting an effect due to increased oxygen supply. Ellis [11] tested the ignition of pine needle beds by glowing barks under the effect of wind. He found that smouldering ignition only appeared in quiescent air, while flaming ignition was observed in windy conditions. For multiple firebrands igniting building materials, the wind velocity was also one of key factors in determining whether the fuel bed would ignite [8]. No ignitions of solid wood products exposed to multiple glowing firebrands occurred at a lower wind speed of 1.3 m/s; however, ignitions were noted at a higher wind speed of 2.4 m/s [8]. Wind is believed to have two competing effects on the combustion of fuel substrate, increasing supply of oxygen and convective cooling, however, the effect of wind on the heat transfer interaction between glowing firebrands and fuel substrate is still less understood.

To better understand the mechanism of glowing firebrand ignition, the measurements of glowing firebrand properties and heat transfer from firebrand to fuel bed, especially in windy environment, are crucial. Some studies have measured the characteristics (for example, surface temperature and radiation heat flux intensity) of glowing firebrands at different wind velocities [14–18]. The results show that the surface temperature and localized heat flux of glowing firebrand increase with an increasing wind, which increases the amount of heat transferred to the fuel bed. Unfortunately, there has not been any systematic experimental study or theory that reveals the role of wind on the combustion characteristics of a glowing firebrand as well as its effect on ignition results. Thus, Urban et al. [19] emphasized that such a study should be conducted to determine rigorously the effect of wind

(like wind velocity, frequency, turbulence intensity, etc.) on the problem of spot ignition by firebrands.

FMC was identified as another important factor to assess the probability of ignition and ignition delay time [7, 20]. Generally, the increase in FMC lead to an increase in ignition delay time, and a decrease in ignition probability [7]. An analytical model, proposed by Yin et al. [21], correlated the ignition delay times (t_{ig}) of pine needle fuels with different FMC through an expression as $t_{ig}^{1/2} \sim FMC$. Urban et al. [19] investigated the effect of FMC on the smouldering ignition of coastal redwood sawdust by glowing firebrands with different sizes. The ignition boundary was qualitatively predicted by using an energy model and found that larger firebrands were capable of igniting sawdust with a higher FMC. In the above analytical models considering the effect of FMC on firebrand ignition, the effect of wind is of little consideration. However, wind effect could couple with FMC effect during the firebrand ignition process. For example, Viegas et al. [20] did not observe ignition by glowing firebrands for a very dry fuel bed without wind, while Yin et al. [21] reported that with 3 m/s ambient wind, ignition of pine needles by a glowing firebrand could occur even if FMC reached 65%. Therefore, the coupling of wind and FMC on glowing frirebrand ignition should be considered.

Thus, the present work seeks to characterize the effect of wind on the ability of a glowing firebrand igniting a moist pine needle fuel bed. The smouldering ignition phenomenon and process were observed. The ignition probability and smouldering ignition delay time were quantified. A heat transfer model was proposed to explain the effect of wind velocity and fuel moisture content on the smouldering ignition delay time.

2. Experimental Methods

2.1. Experimental Setup

All experiments were performed in a laboratory-scale wind tunnel, as depicted in Fig. 1. In the wind tunnel, an axial flow fan (750 W) controlled by a power transducer (range 0 Hz to 50 Hz, resolution 0.1 Hz) provided the desired wind. The wind speed was calibrated with the frequency of the transducers and can range from 0 m/s to 6 m/s. Two layers of damping net and a 10 cm thick honeycomb with 0.52 cm diameter holes were placed in the front of the test section to smooth the airflow. The test section is 120 cm long with a 40 cm by 40 cm cross-section, and had a reinforced glass window on the side for visual observation. A digital video camera (Sony FDR-AXP55, 25 fps) was positioned on the side of the test unit to record the ignition process from a bird's eye view.

One square (slightly larger than 30 cm×30 cm) hole was opened in the floor center of the test section. A rectangular metal basket (30 cm long, 30 cm wide and 6 cm deep), used as fuel container, was placed below this hole. During the experiments, the metal basket, filled with fuels, was lifted so that the fuel's free surface was flush with the floor surface of the test section.
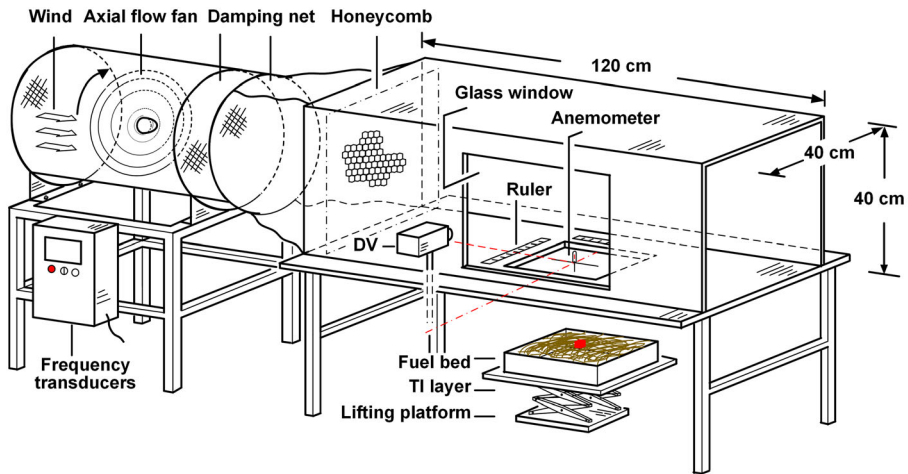
Figure 1. Schematic of the experimental setup. Note that during the ignition test, the upper surface of the fuel bed is lifted and flush with the floor surface of the test section.

A hot-wire anemometer probe (precision: ± 0.02 m/s) measured the wind velocity (U_w) at different positions in the central cross-section of the test section. The standard deviation of wind velocity at different locations is within 10% and the local turbulence velocity fluctuation was less than 6%. In this work, the range of wind velocity was 0 m/s to 4 m/s.

2.2. Materials Preparation

The fuel for this study was pine needles (*Pinus massoniana Lamb*), collected from Sichuan province (southwest China in a humid subtropical climate). This fuel was chosen because pine needles and deciduous leaves, accumulated on the roof or in gutters of buildings are usually typical combustibles to ignite in WUI fires [22]. Otherwise, pine needles are typical receipt fuels for spotting ignition in wildland fires [20, 21].

The diameters of pine needles were around 1 mm and the lengths were within 12 cm to 22 cm. These raw pine needles were dried in air of about 15 ℃ for 15 days, resulting a FMC = $6 \pm 1\%$ in equilibrium with the ambient. Then dead pine needles with different moisture contents were prepared before the experiments with the same procedures mentioned in Ref. [23]. Briefly speaking, (1) firstly, the dead pine needles were dried in an oven at 70 ℃ for 12 h to remove moisture; (2) secondly, the dry pine needles were soaked in warm water for varying lengths of time; (3) thirdly, the water of the pine needles was removed by a commercial vegetable centrifugal dehydrator machine (at a speed of 1000 rpm) and then the pine needles were exposed in air for a while to remove moisture from the surface; (4) finally, the pine needles were stored in sealed bags for more than 48 h to achieve a uniform distribution of moisture. It was observed that there was no obvious water

on the surface of pine needles. Before each test, a small part ($\sim$2.5 g) of the pine needle sample was taken from the fuel bed and the FMC was measured (DHS-20A, Shanghai Lichen-BX Instrument Technology Co. Ltd, the heating temperature is 105 °C). The average moisture contents of the samples used in this study were 5.9%, 14.0%, 19.9%, 30.4%, 41.1%, 53.2% on a dry-mass basis, with the corresponding standard deviations of 1.0%, 1.2%, 2.2%, 1.6%, 1.3%, 1.7%.

The firebrands used in this work were a cube-shape spruce wood (2 cm × 2 cm × 2 cm, density of 397.2 kg/m^3 ± 26.8 kg/m^3). After drying, the moisture content of the firebrand samples was about 3%. In each test, the firebrand was placed in a butane burner flame for 60 s firstly, and then removed and allowed to burn freely for 30 s in quiescent air [21]. The flame of the firebrand was then extinguished by mechanical blowing into a state of glowing combustion, which was consistent with the actual observations [12]. In order to characterize the glowing firebrand, at least 30 prepared glowing firebrands were quenched with water and then dried in an oven at 104 °C for 24 h [24], and the projected area and mass of each firebrand were recorded. After above treatment, the average projected area of the firebrands was 3.97 cm^2 and only approximately 22% of the initial mass remained. The sizes (based on projected area and mass) of the firebrands are consistent with the sizes of firebrands collected from burning trees [25, 26], and aligned with firebrand sizes measured from actual urban fires [27, 28].

2.3. Experimental Procedures

Before each test, the fuel container was filled with the pine needle samples uniformly and then lifted to guarantee the fuel's free surface flushing with the floor of the wind tunnel test section. The dry bulk density of the fuel bed was controlled to be 40 kg/m^3 ± 0.5 kg/m^3, which is consistent with those in hot particle ignition tests [29, 30] and firebrand ignition tests [21]. Once the fuel bed was placed, turned on the fan and the camera. Then, a glowing firebrand was prepared outside the tunnel in quiescent air, and moved into the tunnel through the outlet by a tweezer and dropped on the center of the fuel bed.

Each test resulted in either of two possible outcomes: smouldering ignition or failed ignition. Smouldering ignition was identified if the smouldering combustion of fuel bed became self-sustained, that is, the smouldering front successfully propagated outwards from the firebrand landing region and continued to produce smoke, eventually burnt out the fuel bed. Failed ignition was defined if the smouldering combustion could not propagate over 5 cm in 10 min in any direction, measured with the rulers beside the fuel bed (see Fig. 1), and no longer produce any pyrolyzates.

Setting a criterion to describe the initiation of smouldering ignition is more difficult than flaming ignition. Continuous smoke production is a sign of sustained combustion in pyrolysis materials and has been used as visual evidence of smouldering [8, 21]. The smouldering ignition delay time was defined as the observed delay in the initiation of steady continuous smoke generation and an intensive smouldering combustion. Because of the complexity and randomness of fuel and experiment conditions, 20 to 25 repeated tests were conducted for each set of

experimental conditions to quantify the ignition probability. More than 600 tests were carried out in this work. The ambient temperature was 25 °C±3 °C and the relative humidity was 30% ± 5%.

# 3. Results and Discussion

3.1. Experimental Observation

The ignition outcomes in this study were categorized into two types: smouldering and failed ignition. No direct flaming ignition was observed. In most cases, with the assistance of wind, smouldering ignition transitioned into flaming combustion in this work. Typical cases of smouldering ignition under different wind conditions are illustrated in Fig. 2. As shown in this figure, the successful smouldering ignition by a glowing firebrand can be further divided into three stages: ignition stage (Stage I), self-sustaining smouldering propagation stage (Stage II) and smouldering-to-flaming (StF) transition stage (Stage III). In Stage I, when the firebrand settled on the fuel surface, continuous heat supplied by the firebrand dried and pyrolyzed the nearby fuel, which initiates an exothermic solid-phase reaction of the pine needle fuel bed. Pyrolzate products were clearly visible to flow away from the fuel beds. In Stage II, the initiated solid-phase reaction became self-sustained smouldering and was no longer influenced by heat from the firebrand. In this stage, the charring area on the fuel's surface expanded continuously with a large amount of gas produced. Smouldering spread transitioned into sustained flame spread especially under the assistance of wind [31] in Stage III. In the present work, when the firebrand smouldering ignited the pine needles successfully, the smouldering front continued to spread and transformed into flaming under most windy conditions. Different from a hot metal particle that may act as both the heating source to heat the fuel bed and the pilot source to ignite the pyrolysis gases [32] when igniting fuels, the glowing firebrand here acted as a heating source to initiate smouldering combustion.

To explore the role of wind velocity in the ignition process, Fig. 3 presents four group snapshots of the ignition stage (Stage I) for a fuel bed with FMC of 30.4% ± 1.6% at different U_w. As shown in all snapshots, when landed on the surface of the fuel bed ($t = 0$ s), all the firebrands were burning in a glowing state. When the wind velocity was very low, e.g. 0 m/s and 1 m/s (Fig. 3a), the firebrand was not be able to sustain char oxidation reaction on its surface and extinguished in contact with the relatively cold fuel bed. When the wind velocity became higher, the glowing combustion of the firebrand became remarkably intense in the windward or leading face, and the smouldering ignition occurred near the contact area between the firebrand's windward or leading side and the fuel (the pictures at $t = $ 125 s, 57 s and 41 s in Fig. 3b–d, respectively). Previous work pointed out that the surface temperature of the glowing firebrands increases with increasing air flow [15]. This suggests that the increased wind velocity enhances the heterogeneous combustion (char oxidation) of firebrand and the conductive heat transfer between firebrand and fuel, thereby contributing to fuel bed ignition. Also in Fig. 3b–d, as the wind velocity increased, the ignition position was obvious in a
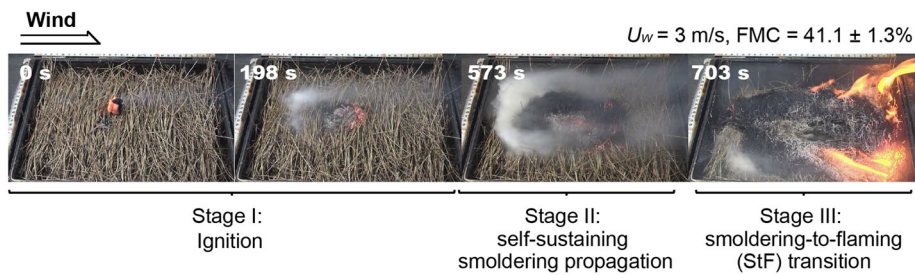
Figure 2.   Three stages of smouldering ignition of a moist pine needle fuel bed by a glowing firebrand at 3 m/s wind velocity.
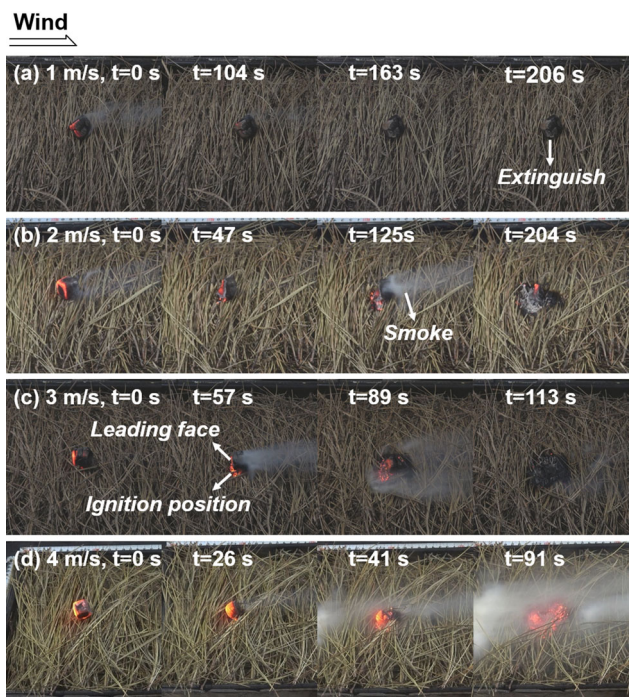
Figure 3.   Four group snapshots of the process of a glowing firebrand igniting pine needle fuel beds with FMC = 30.4% ± 1.6% at different wind velocities: (a) 1 m/s, (b) 2 m/s, (c) 3 m/s and (d) 4 m/s.

more intense smouldering state, which suggests an effect due to increased oxygen supply by air flow.

3.2. Ignition Probability and Ignition Delay Time

As aforementioned before, 20 to 25 repeats were performed for each experimental condition and the outcome of each run was categorized as failed or smouldering

ignition. The ignition probability (P_{ig}), defined as the ratio of successful smouldering ignition number (N_{ig}) to the total testing number (N_{tot}), is expressed as $P_{ig} = N_{ig}/N_{tot}$ and shown in Fig. 4.

With the increase of wind velocity, the ignition probability increases firstly and then decreases. As shown in Fig. 3, the increase of U_w enhances the char oxidation intensity on the firebrand surface by an increased oxygen supply, which releases more energy and promotes the occurrence of ignition ideally. However, the experimental observations demonstrate that even though the firebrands exhibit the strongest glowing state as the U_w increases to 4 m/s, the firebrand mass gradually decreases as the reaction progresses and is likely to be blown away from the fuel bed, ultimately resulting in a decrease in the ignition probability. Moreover, the dilution and diffusion of pyrolysis gas, as well as the enhanced convective cooling in the fuel bed, by external air flow may inhibit the occurrence of direct flaming ignition.

Different from the complicated effect of U_w, the influence of FMC on ignition results is simple. For each U_w, increasing FMC causes a decrease of ignition probability. This is because that the endothermic heating and gasification process of fuel moisture before smouldering initiation acted as a heat loss, whilst wind velocity can promote the combustion chemistry up to the point where the convective losses are more than the heat gains from the enhanced combustion. Figure 4 also shows that a glowing firebrand cannot ignite fuel bed in the absence of wind in this work. Similar results were obtained by Viegas et al. [20] and Eills [33] who also did not observe ignition by glowing firebrands without wind.
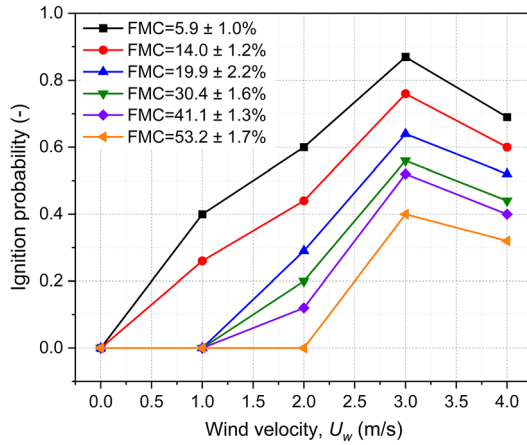
The smouldering ignition delay time was defined as the interval between the moment when the firebrand landed on the fuel bed ($t = 0$ s) and when the featured phenomenon of smouldering ignition appeared. Figure 5 shows the smouldering ignition delay times of the pine needle fuel beds under different wind velocities. Different from the ignition probability, the ignition delay time shows a monotonic decrease with the increase of U_w under the same FMC. It is seen that an increase of FMC leads to an increase of ignition delay time because of the additional time necessary to dry the fuel.

3.3. Theoretical Analysis

In this work, a glowing firebrand could initiate smouldering of the moist pine needle fuel bed. Under most successful smoldering ignition conditions, smoldering ignition occurred in the area of the fuel bed near the lower part of the leading face of the firebrand. Continued heat supplied from the firebrand contributed to initiate an exothermic solid-phase reaction of fuels, leading to smoldering ignition. Here we presented a theoretical analysis on heat transfer process between the firebrand and the fuel bed and provided an explanation on the influences of both wind velocity and fuel moisture content on the ignition results.

To accurately represent the ignition process, two aspects, the heat required for fuel ignition and the heat transferred from firebrands to fuels, were considered. In general, the required duration for smoldering ignition (t_{ig}) is the time required to heat the fuel to a critical smoldering ignition temperature (T_{sm}), which is the

Figure 4. Ignition probability of the moist pine needle fuel bed by a glowing firebrand under the influence of ambient wind.
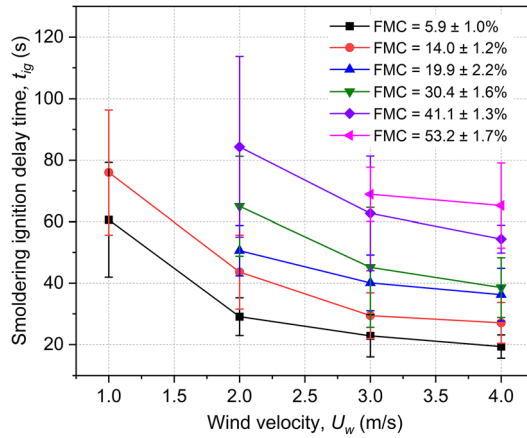
Figure 5. Smouldering ignition delay time for the ignition of moist pine needle fuel bed by a glowing firebrand under the influence of ambient wind.

threshold temperature of char oxidation [34]. To successfully ignite the fuel bed, $Q_{fb,trans} \geq Q_{ig}$ is required, where $Q_{fb,trans}$ is the heat transferred from the glowing firebrand to the fuel and Q_{ig} is the heat required for the smoldering ignition of the fuel. Assuming ignition occurs when the temperature of the fuel bed reaches T_{sm}, Q_{ig} may be described as

$$Q_{ig} = V_F \rho_F \left[c_{p,F}(T_{sm} - T_0) + FMC \cdot \Delta h_{vap} \right] \tag{1}$$

where ρ_F, $c_{p,F}$ and T_0 are the bulk density, specific heat capacity and initial temperature of the dry fuel bed, respectively. The energy required to bring the moisture in the fuel from T_0 to saturated steam is Δh_{vap}, which accounts for both the sensible enthalpy and the heat of evaporation (kJ/kg). V_F is the volume of fuel involved in ignition and can be approximated by the contact area ($A_{contact}$) between the firebrand and the fuel bed multiplied by the penetrated depth (δ) of fuel due to firebrand heating [10, 21], which is expressed as [35]

$$\delta = \sqrt{\alpha t_{ig}} = \sqrt{\frac{k}{\rho_F c_{p,F}} t_{ig}} \tag{2}$$

where, α and k are the thermal diffusivity and thermal conductivity of the fuel bed, respectively. It is noted that the penetrated depth is proposed for solid fuels, but here is used for porous fuel bed, assuming that the fuel bed acts as an effective solid.

Then Eq. (1) can be rewritten as

$$Q_{ig} \approx A_{contact} \sqrt{\frac{\rho_F k}{c_{p,F}} t_{ig}} \cdot \left[c_{p,F}(T_{sm} - T_0) + FMC \cdot \Delta h_{vap} \right] \tag{3}$$

As a glowing firebrand is exposed to the air flow, heterogeneous surface oxidation reactions take place, which heat the fuel. The heat transferred from the glowing firebrand to the fuel ($Q_{fb,trans}$) can be calculated as the difference between the combustion heat release ($Q_{fb,coms}$) and the heat loss to the ambient ($Q_{fb,loss}$)

$$\begin{aligned} Q_{fb,trans} &\approx Q_{fb,coms} - Q_{fb,loss} \\ &= \beta \dot{m}_c \Delta H_c t_{ig} - A_{s,fb} t_{ig} \left[h_{c,fb}(T_{fb} - T_\infty) + \varepsilon \sigma(T_{fb}^4 - T_\infty^4) \right] \end{aligned} \tag{4}$$

where $\beta = 1 - \varphi$, φ is the energy released from the char oxidation reaction that is absorbed by the firebrand. Only a portion, 0.285 [15, 36], of the energy released by the reaction is absorbed by the firebrand. $\dot{m}_c$ is the mass loss rate of char, ΔH_c is the heat of combustion of the char oxidation (kJ/kg), $h_{c,fb}$ is the convective heat transfer coefficient, ε is the firebrand surface emissivity, σ is the Stefan–Boltzmann constant, T_{fb} and T_∞ are the firebrand surface temperature and ambient temperature.

Since the aspect ratio of the firebrand is unity and visual observation (Fig. 3c and d) showed that the leading face of the firebrand tended to be rounded gradually as it burned, we can assume that the firebrand is effectively a sphere with the diameter of d_{fb}. Then the convective heat transfer coefficient $h_{c,fb}$ can be calculated based on d_{fb} by using a Nusselt number correlation for a sphere [15]

$$h_{c,fb} = (Nu \cdot k_{air})/d_{fb} \tag{5}$$

where k_{air} is the thermal conductivity of air. The local Nusselt number is calculated with the empirical expression below (Eq. (6)) for flow over a sphere [37], and the Reynolds number in this expression is expressed as Eq. (7).

$$Nu = 2 + 1.31Re^{1/2}Pr^{1/3} \tag{6}$$

$$Re = U_w \rho d_{fb}/\mu \tag{7}$$

where Pr, μ and ρ are the Prandtl number, kinematic viscosity and density of air, respectively. In the range of wind velocity (0 m/s to 4 m/s) in this study, the Re numbers are from 0 to 5113.

In Eq. (4), the two most important parameters are $\dot{m}_c$ and T_{fb}. Visual observation showed that under different U_w, the firebrand exhibited different combustion characteristics, that is, different mass loss rates and surface temperatures. Surface char oxidation is dependent on the transport of oxygen to the char surface. Same with previous burning rate models of glowing firebrands [14, 15], we can assume that the rate is dominated by convective mass transfer of oxygen to the surface. Visual observation also showed that only half the firebrand was exposed to the surrounding air and the diameter of the firebrand remains almost unchanged during the ignition process, the effective firebrand surface area (m^2) where glowing combustion occurred was assumed half of the firebrand surface area, $A_{s,fb} = \pi d_{fb}^2/2$. Then the mass loss rate of char was expressed as

$$\dot{m}_c = A_{s,fb} h_m \left(\frac{Y_{O2,i}}{r_o} \right) = \pi d_{fb}^2 \rho h_m \left(\frac{Y_{O2,i}}{r_o} \right)/2 \tag{8}$$

where h_m is the mass transfer coefficient of oxygen (m/s), $Y_{O2,i}$ is the oxygen mass fraction in air (0.233). In Eq. (8), it is assumed that all oxygen transported to the surface is consumed by char oxidation. r_o is the oxygen-to-fuel ratio and equals 2.664 for all combustion products being CO_2 [38].

Since the governing equations for heat transfer and mass transfer are similar, the dimensionless terms controlling heat transfer and mass transfer can be equated. So the mass transfer coefficient can be correlated with the convective heat transfer coefficient $h_{c,fb}$ as mentioned by Lattimer et al. [14]

$$h_m = \frac{h_{c,fb}}{\rho c_{p,air} Le^{2/3}} \tag{9}$$

where Le is the Lewis number of air. Le is usually 1.0 for simplification and thus the mass transfer coefficient is

$$h_m = \frac{h_{c,fb}}{\rho c_{p,air}} \tag{10}$$

The mass loss rate of char can be calculated by using Eqs. (8) and (10). With the assumptions that only a portion of the energy released by the reaction is absorbed by the firebrand and the surface area of the firebrand was assumed to be half that of a sphere, the temperature of the leading face of the firebrand can be calculated by balancing the energy equation on the surface of the firebrand, as

$$\varphi \dot{m}_c \Delta H_c - A_{s,fb} \varepsilon \sigma \left[T_{fb}^4 - T_\infty^4 \right] - A_{s,fb} h_{c,fb} \left(T_{fb} - T_\infty \right) = 0 \tag{11}$$

Substituting Eq. (11) in to Eq. (4), $Q_{fb,trans}$ can be rewritten as

$$Q_{fb,trans} = (1 - 2\varphi) \dot{m}_c \Delta H_c \tag{12}$$

which means about 43% of heat released by firebrand combustion is retained by the fuels.

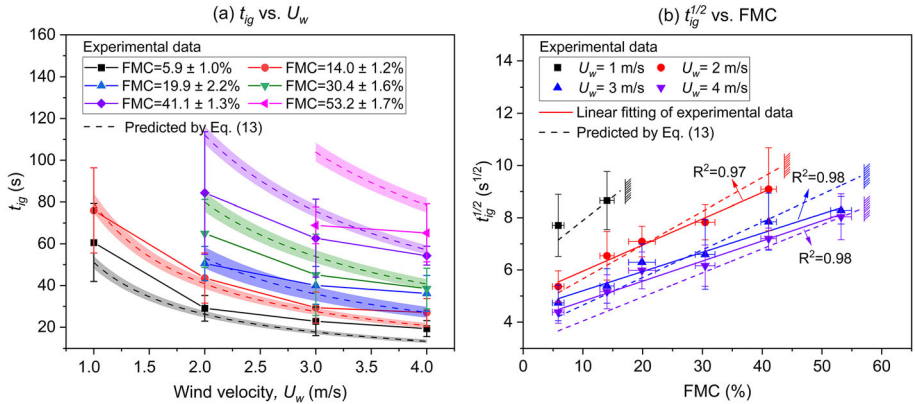With Eqs. (1) and (12), the smoldering ignition delay time t_{ig} can express as

$$t_{ig}^{1/2} \approx \frac{A_{contact} \sqrt{\frac{\rho_F k}{c_{p,F}}} \left[c_{p,F}(T_{sm} - T_0) + FMC \cdot \Delta h_{vap} \right]}{(1 - 2\varphi) \dot{m}_c \Delta H_c} \tag{13}$$

Equation (13) indicates that the square root of smoldering ignition delay time linearly correlates with FMC at the same U_w, which is consistent with the results of Yin et al. [21]. Wind affects the ignition results by affecting the combustion rate of the firebrands ($\dot{m}_c$). By using the parameter values in Table 1, the smoldering ignition delay time can be predicted theoretically by Eq. (13), which is presented in Fig. 6, together with the experimental data.

The effect of wind velocity on the smouldering ignition delay time is shown in Fig. 6a. The dotted line is the ignition delay time with average FMC, and the shaded areas around the dotted lines indicate the ignition delay time change caused by the standard deviation of FMC. Overall, the model predicted the variation trend of the smoldering ignition delay time with the wind velocity well when FMC was less than 20%. However, at high FMC, the predicted variation trend diverged from the experimental data, which may be because FMC would affect the heat transfer characteristics of the fuel bed, and thus affect the heat transfer to the fuel bed. Furthermore, under a certain wind velocity, a linear relationship between $t_{ig}^{1/2}$ (experimental data) and FMC is observed and also proved by the model predictions in Fig. 6b. Note that Eq. (13) is an approximate expression, not an exact equation. So the theoretical prediction by Eq. (13) gives the variation trend of the smoldering ignition delay time with the FMC and wind velocity, not exactly predict the experimental values.

Table 1
Physical Parameters and Values

Parameter	Symbol	Value
Bulk density of fuel bed	ρ_F	40 kg/m^3
Specific heat capacity of fuel	$c_{p,F}$	1.470 kJ/(kg K) [39]
Heat of water evaporation	Δh_{vap}	2570 kJ/kg [21]
Contact area between the firebrand and the fuel	$A_{contact}$	2×10^{-4} m^2
Thermal conductivity of the pine needles	k	0.11 W/(m K) [40]
Characteristic smoldering temperature	T_{sm}	500 °C [29]
Initial temperature of fuel bed	T_0	298 K
Combustion heat of char oxidation (all combustion products being CO_2)	ΔH_c	32,793 kJ/kg [14]
Temperature of ambient air	T_∞	298 K
Thermal conductivity of air at 300 K	k_{air}	2.63×10^{-5} kW/(m K) [14]
Prandtl number for air at 300 K	Pr	0.707 [14]
Kinematic viscosity of air at 300 K	μ	1.846×10^{-5} N s/m^2 [14]
Specific heat capacity of air at 300 K	$c_{p,air}$	1.084 kJ/(kg K) [14]
Density of air at 298 K	ρ	1.18 kg/m^3 [14]

Figure 6. **Comparison of the experimental and predicted values of the smouldering ignition delay time. (a) effect of wind velocity (U_w). The dotted lines represent the calculated values of the model and the shaded areas around the dotted lines are caused by the standard deviation of FMC. (b) effect of FMC. The linear relationship between $t_{ig}^{1/2}$ and FMC is verified.**

4. Conclusion

In this study, more than 600 experiments were performed to gain insight into the effect of wind on smouldering ignition of moist pine needles by a glowing firebrand. The ignition process, ignition probability, smouldering ignition delay time were evaluated at five different wind velocities in the range of zero to 4 m/s and six fuel moisture contents (FMC) in the range of 5.9 to 53.2%. Based on the performed experiments and analysis, it is possible to draw the following specific conclusions.

(1) A glowing firebrand could initiate smouldering of the fuel bed, and can transition to flaming combustion with the assistance of wind. Wind has a significant impact on the ignition process by affecting the combustion state of the firebrand. As the wind velocity increases, the ignition probability firstly increases and then decreases, but the smouldering ignition delay time decreases. As FMC increases, the ignition probability decreases, but the smouldering ignition delay time increases.

(2) Based on heat transfer between the firebrand and fuel bed, a theoretical model was proposed to predict the relationship of the smouldering ignition delay time with the ambient wind velocity and the fuel moisture content. Overall, the model predicted the variation trend of the smoldering ignition delay time with the wind velocity well when FMC was less than 20%, but poor at higher FMC. It is found that wind affects the ignition results by affecting the combustion rate of the firebrand and wind velocity has a nonlinear effect on the ignition delay time, while the square root of ignition delay time has a good linear relationship with FMC.

This study deepens the understanding of firebrand ignition and expounds on the important role of wind in the ignition process. It is desired that these results, in conjunction with other literature studies, could be used to validate firebrand ignition models.

Declarations

Competing Interests   The authors declare that they have no known competing financial interests or personal relationships that could have appeared to influence the work reported in this paper.

References

1. Bowman DM, Williamson GJ, Abatzoglou JT, Kolden CA, Cochrane MA, Smith AM (2017) Human exposure and sensitivity to globally extreme wildfire events. Nat Ecol Evol 1:0058. https://doi.org/10.1038/s41559-016-0058

2. Hammer RB, Radeloff VC, Fried JS, Stewart SI (2007) Wildland-urban interface housing growth during the 1990s in California, Oregon, and Washington. Int J Wildland Fire 16:255–265. https://doi.org/10.1071/WF05077

3. Jolly WM, Cochrane MA, Freeborn PH, Holden ZA, Brown TJ, Williamson GJ, Bowman DM (2015) Climate-induced variations in global wildfire danger from 1979 to 2013. Nat Commun 6:7537. https://doi.org/10.1038/ncomms8537

4. Blanchi R, Maranghides A, England JR (2020) Lessons learnt from post-fire surveys and investigations. In: Manzello SL (ed) Encyclopedia of Wildfires and Wildland-Urban Interface (WUI) fires Springer, Cham, pp 743–756

5. Mell WE, Manzello SL, Maranghides A, Butry D, Rehm RG (2010) The wildland-urban interface fire problem—current approaches and research needs. Int J Wildland Fire 19:238–251. https://doi.org/10.1071/WF07131

6. Fernandez-Pello AC (2017) Wildland fire spot ignition by sparks and firebrands. Fire Saf J 91:2–10. https://doi.org/10.1016/j.firesaf.2017.04.040

7. Ganteaume A, Lampin-Maillet C, Guijarro M, Hernando C, Jappiot M, Fonturbel T, Perez-Gorostiaga P, Vega JA (2009) Spot fires: fuel bed flammability and capability of firebrands to ignite fuel beds. Int J Wildland Fire 18:951–969. https://doi.org/10.1071/WF07111

8. Manzello SL, Park SH, Cleary TG (2009) Investigation on the ability of glowing firebrands deposited within crevices to ignite common building materials. Fire Saf J 44:894–900. https://doi.org/10.1016/j.firesaf.2009.05.001

9. Salehizadeh H (2019) Critical ignition conditions of structural materials by cylindrical firebrands. Dissertation, University of Maryland

10. Wessies SS, Chang MK, Marr KC, Ezekoye OA (2019) Experimental and analytical characterization of firebrand ignition of home insulation materials. Fire Technol 55:1027–1056. https://doi.org/10.1007/s10694-019-00818-8

11. Ellis PFM (2011) Fuelbed ignition potential and bark morphology explain the notoriety of the eucalypt messmate 'stringybark' for intense spotting. Int J Wildland Fire 20:897–907. https://doi.org/10.1071/WF10052

12. Tarifa C, Del Notario P, Moreno F, Villa A (1967) Transport and combustion of firebrands, instituto nacional de tecnica aeroespacial, Report No. Grants FG-SP-114 and FG-SP-146

13. Waterman T, Takata A (1969) Laboratory study of ignition of host materials by firebrands, IIT Research Institute, Report No. IITRI-j6142

14. Lattimer BY, Bearinger E, Wong S, Hodges JL (2022) Evaluation of models and important parameters for firebrand burning. Combust Flame 235:111619. https://doi.org/10.1016/j.combustflame.2021.111619

15. Urban JL, Vicariotto M, Dunn-Rankin D, Fernandez-Pello AC (2019) Temperature Measurement of Glowing Embers with Color Pyrometry. Fire Technol 55:1013–1026. https://doi.org/10.1007/s10694-018-0810-3

16. Kim DK, Sunderland PB (2019) Fire ember pyrometry using a color camera. Fire Saf J 106:88–93. https://doi.org/10.1016/j.firesaf.2019.04.006

17. Hakes RSP, Salehizadeh H, Weston-Dawkes MJ, Gollner MJ (2019) Thermal characterization of firebrand piles. Fire Saf J 104:34–42. https://doi.org/10.1016/j.firesaf.2018.10.002

18. Bearinger ED, Hodges JL, Yang F, Rippe CM, Lattimer BY (2020) Localized heat transfer from firebrands to surfaces. Fire Saf J . https://doi.org/10.1016/j.firesaf.2020.103037

19. Urban JL, Song J, Santamaria S, Fernandez-Pello C (2019) Ignition of a spot smolder in a moist fuel bed by a firebrand. Fire Saf J 108:102833. https://doi.org/10.1016/j.firesaf.2019.102833

20. Viegas DX, Almeida M, Raposo J, Oliveira R, Viegas CX (2014) Ignition of mediterranean fuel beds by several types of firebrands. Fire Technol 50:61–77. https://doi.org/10.1007/s10694-012-0267-8

21. Yin P, Liu N, Chen H, Lozano JS, Shan Y (2014) New correlation between ignition time and moisture content for pine needles attacked by firebrands. Fire Technol 50:79–91. https://doi.org/10.1007/s10694-012-0272-y

22. Puchovsky M, Simeoni A, Han E, Parrow D, Rozen A (2020) The feasibility of protecting residential structures from wildfires using a fixed exterior fire fighting system, E-project-041020-153548

23. Zhang H, Qiao Y, Chen H, Liu N, Zhang L, Xie X (2020) Experimental study on flaming ignition of pine needles by simulated lightning discharge. Fire Saf J 120:103029. https://doi.org/10.1016/j.firesaf.2020.103029

24. Suzuki S, Manzello SL (2019) Investigating effect of wind speeds on structural firebrand generation in laboratory scale experiments. Int J Heat Mass Transf 130:135–140. https://doi.org/10.1016/j.ijheatmasstransfer.2018.10.045

25. Manzello SL, Maranghides A, Mell WE (2007) Firebrand generation from burning vegetation. Int J Wildland Fire 16:458–462. https://doi.org/10.1071/WF06079

26. Manzello SL, Maranghides A, Shields JR, Mell WE, Hayashi Y, Nii D (2009) Mass and size distribution of firebrands generated from burning Korean pine (*Pinus koraiensis*) trees. Fire Mater 33:21–31. https://doi.org/10.1002/fam.977

27. Suzuki S, Manzello SL (2021) Firebrands generated in Shurijo castle fire on October 30th, 2019. Fire Technol 58:777–791. https://doi.org/10.1007/s10694-021-01176-0

28. Suzuki S, Manzello SL (2018) Characteristics of firebrands collected from actual urban fires. Fire Technol 54:1533–1546. https://doi.org/10.1007/s10694-018-0751-x

29. Wang S, Huang X, Chen H, Liu N (2017) Interaction between flaming and smouldering in hot-particle ignition of forest fuels and effects of moisture and wind. Int J Wildland Fire 26:71–81. https://doi.org/10.1071/WF16096

30. Fang W, Peng Z, Chen H (2021) Ignition of pine needle fuel bed by the coupled effects of a hot metal particle and thermal radiation. Proc Combust Inst 38:5101–5108. https://doi.org/10.1016/j.proci.2020.05.032

31. Rein G (2016) Smoldering combustion. In: Hurley MJ, Gottuk D, Hall JR, Harada K, Kuligowski E, Puchovsky M, Torero J, Watts JM, Wieczorek C (eds) SFPE handbook of fire protection engineering Springer, New York, pp 581–603

32. Wang S, Huang X, Chen H, Liu N, Rein G (2015) Ignition of low-density expandable polystyrene foam by a hot particle. Combust Flame 162:4112–4118. https://doi.org/10.1016/j.combustflame.2015.08.017

33. Ellis PF (2000) The aerodynamic and combustion characteristics of eucalypt bark : a firebrand study. Dissertation, Australian National University

34. Lin S, Sun P, Huang X (2019) Can peat soil support a flaming wildfire?. Int J Wildl Fire 28:601–613. https://doi.org/10.1071/WF19018

35. Quintiere JG (2006) Fundamentals of fire phenomena. Wiley, Chichester

36. Sardoy N, Consalvi JL, Porterie B, Fernandez-Pello AC (2007) Modeling transport and combustion of firebrands from burning trees. Combust Flame 150:151–169. https://doi.org/10.1016/j.combustflame.2007.04.008

37. Galloway TR, Sage BH (1968) Thermal and material transfer from spheres: Prediction of local transport. Int J Heat Mass Transf 11:539–549. https://doi.org/10.1016/0017-9310(68)90095-1
38. Turns SR (2012) An Introduction to Combustion: Concepts and Applications. New York
39. Consalvi JL, Nmira F, Fuentes A, Mindykowski P, Porterie B (2011) Numerical study of piloted ignition of forest fuel layer. Proceedings of the Combustion Institute 33:2641–48. https://doi.org/10.1016/j.proci.2010.06.025
40. Tihay V, Simeoni A, Santoni PA, Rossi L, Garo JP, Vantelon JP (2009) Experimental study of laminar flames obtained by the homogenization of three forest fuels. Int J Therm Sci 48:488–501. https://doi.org/10.1016/j.ijthermalsci.2008.03.018